Calcium homeostasis modulator 1 (CALHM1) is the pore-forming subunit of an ion channel that mediates extracellular Ca^{2+} regulation of neuronal excitability

Zhongming Ma[a], Adam P. Siebert[a], King-Ho Cheung[a], Robert J. Lee[a], Brian Johnson[b], Akiva S. Cohen[b,c], Valérie Vingtdeux[d], Philippe Marambaud[d], and J. Kevin Foskett[a,e,1]

Departments of [a]Physiology, [c]Pediatrics, and [e]Cell and Developmental Biology, University of Pennsylvania, Philadelphia, PA 19104; [b]Division of Neurology, Children's Hospital of Philadelphia, Philadelphia, PA 19104; and [d]Litwin–Zucker Research Center for the Study of Alzheimer's Disease, The Feinstein Institute for Medical Research, North Shore–Long Island Jewish Health System, Manhasset, NY 11030

Edited by Richard W. Aldrich, University of Texas at Austin, Austin, TX, and approved May 18, 2012 (received for review March 9, 2012)

Extracellular Ca^{2+} (Ca^{2+}_o) plays important roles in physiology. Changes of Ca^{2+}_o concentration ($[Ca^{2+}]_o$) have been observed to modulate neuronal excitability in various physiological and pathophysiological settings, but the mechanisms by which neurons detect $[Ca^{2+}]_o$ are not fully understood. Calcium homeostasis modulator 1 (CALHM1) expression was shown to induce cation currents in cells and elevate cytoplasmic Ca^{2+} concentration ($[Ca^{2+}]_i$) in response to removal of Ca^{2+}_o and its subsequent addback. However, it is unknown whether CALHM1 is a pore-forming ion channel or modulates endogenous ion channels. Here we identify CALHM1 as the pore-forming subunit of a plasma membrane Ca^{2+}-permeable ion channel with distinct ion permeability properties and unique coupled allosteric gating regulation by voltage and $[Ca^{2+}]_o$. Furthermore, we show that CALHM1 is expressed in mouse cortical neurons that respond to reducing $[Ca^{2+}]_o$ with enhanced conductance and action potential firing and strongly elevated $[Ca^{2+}]_i$ upon Ca^{2+}_o removal and its addback. In contrast, these responses are strongly muted in neurons from mice with *CALHM1* genetically deleted. These results demonstrate that CALHM1 is an evolutionarily conserved ion channel family that detects membrane voltage and extracellular Ca^{2+} levels and plays a role in cortical neuronal excitability and Ca^{2+} homeostasis, particularly in response to lowering $[Ca^{2+}]_o$ and its restoration to normal levels.

Alzheimer's disease | mutagenesis | selectivity | neurodegeneration | polymorphism

Originally identified as a possible modifier of the age of onset of Alzheimer's disease (1, 2), *calcium homeostasis modulator 1* (*CALHM1*) encodes a glycosylated membrane protein expressed throughout the brain that lacks homology to other proteins. Six human CALHM homologs have been identified, with alternatively spliced variants and different expression patterns throughout the body, and CALHM1 is conserved across >20 species. Expression of recombinant human CALHM1 in mammalian cells was found to strongly influence processing of amyloid precursor protein to amyloid beta (Aβ) under an experimental protocol that involved removal of Ca^{2+}_o for several minutes and its subsequent restoration to the bathing medium (1). This procedure resulted in a large rise of $[Ca^{2+}]_i$. Accordingly, it was speculated that CALHM1 influences Aβ production by altering cellular Ca^{2+} homeostasis. CALHM1 was found to homo-multimerize and it was speculated that it might function as an ion channel component or regulator of membrane ion conductances (1). Nevertheless, neither the functions of CALHM1 nor those of any of the other members of this gene family are known. Here we have identified CALHM1 as the pore-forming subunit of a unique plasma membrane Ca^{2+}-permeable ion channel. Furthermore, we demonstrate that CALHM1 is regulated by both voltage and extracellular $[Ca^{2+}]$. Extracellular Ca^{2+} regulates an intrinsic voltage-dependent gating mechanism, increasing the voltage dependence and stabilizing the channel in the closed state. Mouse cortical neurons express CALHM1 and respond to lowering $[Ca^{2+}]_o$ with enhanced conductance and action potential firing and strongly elevated $[Ca^{2+}]_i$ upon Ca^{2+}_o removal and its subsequent addback. In contrast, these responses are nearly abolished in neurons from mice with *CALHM1* genetically deleted. Thus, CALHM1 is a voltage- and extracellular Ca^{2+}-gated neuronal Ca^{2+}-permeable ion channel that regulates cortical neuronal excitability in response to reduced extracellular Ca^{2+} concentrations.

Results

CALHM1 Expression Induces a Voltage-Dependent Plasma Membrane Conductance. Previously, outwardly rectified ion currents were observed in CALHM1-expressing *Xenopus* oocytes and CHO cells by a slow voltage ramp protocol (1). However, those experiments did not establish whether CALHM1 is an essential component of an underlying ion channel(s), accessory protein, or actual pore-forming subunit. Furthermore the detailed permeation and gating properties of the conductance were not determined. In addition, precautions were not taken to fully ensure lack of contribution of endogenous conductances. To distinguish whether CALHM1 is a unique ion channel or a regulator of endogenous channels, plasma membrane currents were recorded in *Xenopus* oocytes under conditions that minimized contributions of endogenous conductances (Fig. S1) (3, 4). Membrane depolarization in solutions containing 2 mM Ca^{2+} and 1 mM Mg^{2+} generated large outward currents that activated slowly ($\tau \sim 3.11 \pm 0.28$ s at +60 mV; $n = 10$) and deactivated at hyperpolarized voltages ($\tau = 0.204 \pm 0.022$ s at −80 mV; $n = 10$) specifically in CALHM1-expressing oocytes (Fig. 1*A*). Expression of CALHM1-EGFP localized to the plasma membrane (Fig. 1*B*). Similar results were obtained in transiently transfected N2A mammalian neuroblastoma cells (Fig. 1*C*). Thus, expression of CALHM1 induced a voltage-dependent plasma membrane conductance.

The monovalent ion permeabilities of this conductance were estimated by changing-bath [NaCl] in a nominally 0-Ca^{2+} solution (free $[Ca^{2+}]$ ~10 μM) and measuring shifts of reversal potential, ΔE_{rev} (Fig. 1*D*). Using the Goldman–Hodgkin–Katz (GHK) constant field equation, the relative permeabilities were estimated as $P_{Na}:P_K:P_{Cl} = 1:1.17:0.56$. Similar results were obtained with bath Na^+ replaced by K^+ in either 0 or 2 mM Ca^{2+}_o.

Author contributions: Z.M., B.J., A.S.C., and J.K.F. designed research; Z.M., A.P.S., K.-H.C., R.J.L., V.V., and P.M. performed research; Z.M., B.J., A.S.C., and J.K.F. analyzed data; and Z.M. and J.K.F. wrote the paper.

The authors declare no conflict of interest.

This article is a PNAS Direct Submission.

[1]To whom correspondence should be addressed. E-mail: foskett@mail.med.upenn.edu.

See Author Summary on page 11080 (volume 109, number 28).

This article contains supporting information online at www.pnas.org/lookup/suppl/doi:10.1073/pnas.1204023109/-/DCSupplemental.

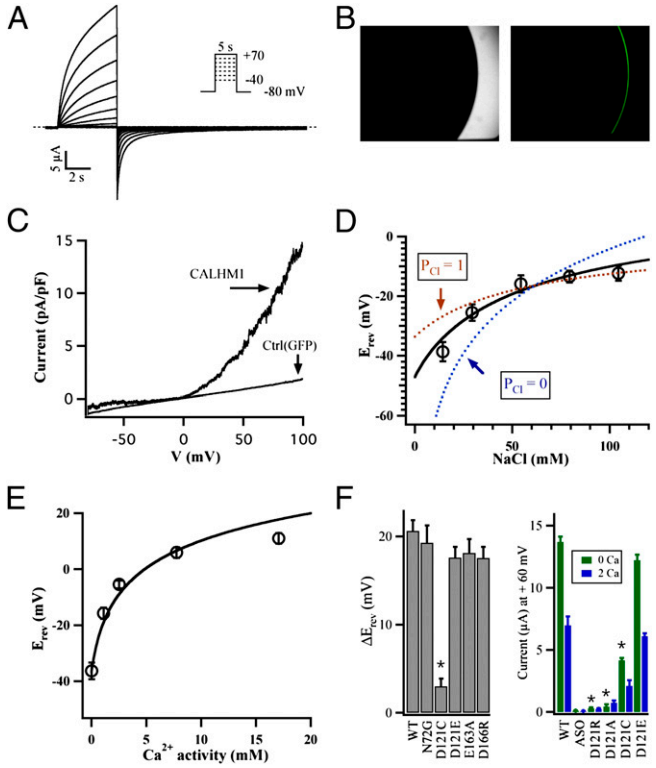

Fig. 1. CALHM1 is a Ca^{2+}-selective ion channel. (*A*) Family of currents evoked in CAHLM1-expressing oocyte in response to voltage pulses from holding potential of −80 mV in a solution containing 2 mM Ca^{2+} and 1 mM Mg^{2+} every 60 s. (*B*) CALHM1-GFP expressed in plasma membrane of *Xenopus* oocyte. (*Left*) Transmitted light image; (*Right*) confocal fluorescence image at oocyte equator demonstrating plasma membrane localization of CALHM1-GFP. (*C*) Whole-cell currents measured in control GFP- (n = 4) and CALHM1 (n = 5)-expressing N2A cells by a voltage-ramp protocol from −80 to +100 mV over 5 s (−60 mV holding potential) in bath solution containing 1.5 mM Ca^{2+} and 1 mM Mg^{2+}. (*D*) Reversal potentials (E_{rev}) measured over a range of bath [NaCl] in nominal absence of divalent cations (n = 9 oocytes). Solid line is GHK constant field equation fit with the relative permeability ratios P_{Na}:P_K:P_{Cl} = 1:1.17:0.56. Two dashed lines are GHK constant field equation fits with the fixed relative permeability of Cl^- to 0 and 1, respectively. (*E*) E_{rev} measured in range of bath Ca^{2+} activities (n = 5). Solid line is extended GHK equation fit with P_{Ca}:P_{Na} = 10.9. (*F*) Changes in E_{rev} measured as in *E* (*Left*) and currents (*Right*) (same amount of cRNAs injected) in response to changing $[Ca^{2+}]_o$ from 0 to 2 mM in oocytes expressing WT and mutant CALHM1. n = 3–6, mean ± SEM; *Student's t test, $P < 0.05$.

Replacement of 90 mM Cl^- in oocytes bathed in 100 mM NaCl solution with an equal concentration of methanesulfonate (Mes^-) reversibly shifted ΔE_{rev} by 6.3 ± 0.8 mV (n = 6), confirming the substantial Cl^- permeability. Thus, the CALHM1-induced conductance has monovalent permeability with relatively minor selectivity for cations over chloride. Increasing $[Ca^{2+}]_o$ in constant [NaCl] shifted E_{rev} to more positive voltages (Fig. 1*E*), indicating a relative permeability ratio P_{Ca}:P_{Na} ~ 11. Thus, CALHM1 currents are Ca^{2+}, monovalent cation, and chloride permeable with selectivity Ca^{2+} >> Na^+ ~ K^+ > Cl^-.

CALHM1 Is the Pore-Forming Subunit of a Plasma Membrane Ion Channel. To establish whether CALHM1 is itself a plasma membrane ion channel, we evaluated the relative Ca^{2+} selectivity of CALHM1 containing single-point mutations. It was noted that CALHM1 possesses a sequence similar to that of the ion selectivity filters of NMDA receptors (NMDAR) (1), including an asparagine at position 72 (Asn72) near the cytoplasmic end of putative TM2. Nevertheless, ΔE_{rev} in response to changing $[Ca^{2+}]_o$ from 0 to 2 mM was not different between wild-type (WT) and CALHM1 with Asn72 mutated to glycine (N72G; Fig. 1*F* and Fig. S2). Furthermore, current magnitudes in N72G- and WT-CALHM1–expressing oocytes were similar. These results indicate that Asn72 does not contribute to Ca^{2+} selectivity and suggest that CALHM1 lacks structural similarity with the NMDAR pore region. Acidic residues are important determinants of ion permeation through Ca^{2+} channels (5, 6). CALHM1 is predicted to have four transmembrane helices, similar to ORAI Ca^{2+} channels (7), where acidic residues near the end of transmembrane helices and in extracellular loops play key roles in ion permeation (7, 8). Mutation of either Glu163 (E163A) or Asp166 (D166R) in the putative second extracellular loop of CALHM1 was without effect (Fig. 1*F*). In contrast, mutation of Asp121, predicted to lie at the extracellular end of putative TM3, to Cys (D121C) eliminated the ΔE_{rev} response to changing $[Ca^{2+}]_o$ (Fig. 1*F* and Fig. S2). ΔE_{rev} was restored to normal in D121E CALHM1, which preserves the negative charge (Fig. 1*F*). Mutation of this residue to Arg, to reverse the charge, completely abolished CALHM1 ion currents (Fig. 1*F*). These results indicate that D121 contributes not only to Ca^{2+} selectivity, but also to the conductance pathway for other ions. Together, these results demonstrate that CALHM1 itself forms a unique plasma membrane ion channel and suggest that the extracellular end of putative TM3 lines the CALHM1 ion pore.

CALHM1 Is Activated by Lowering Extracellular Calcium. Removal and subsequent addback of $Ca^{2+}{}_o$ strongly elevated $[Ca^{2+}]_i$ in CALHM1-expressing N2A (Fig. 2*A* and Fig. S3*C*) cells, as shown previously in other cells (1, 9). To examine the relationship between this $[Ca^{2+}]_i$ response and CALHM1 channel activity, CALHM1-expressing oocytes were bathed in a Ca^{2+} solution lacking Mg^{2+} and voltage clamped at a holding potential of −15 mV. Exposure to a divalent cation-free solution reversibly induced large inward currents at −80 mV in a concentration- and time-dependent manner (Fig. 2 *B* and *C*). Reducing bath $[Ca^{2+}]$ over a range of concentrations revealed a half-maximal $Ca^{2+}{}_o$ activation concentration (IC_{50}) of 221 μM with a Hill coefficient of 2.1, indicating that CALHM1 is strongly regulated by $[Ca^{2+}]_o$ (Fig. 2 *C* and *D*). $Mg^{2+}{}_o$ also regulated CALHM1 channel gating, but with 10-fold lower affinity (IC_{50} = 3.26 mM; Hill coefficient = 2.3) (Fig. 2*D*). The dose–response relation for Mg^{2+} is similar in shape to that of Ca^{2+} at the same holding potential, suggesting that both cations bind to the same site and regulate channel gating by a similar mechanism. Expression of CALHM1 in N2A cells also induced voltage- and $Ca^{2+}{}_o$-gated currents (Fig. 2 *E* and *F*). Thus, regulation of CALHM1 gating by voltage and $Ca^{2+}{}_o$ is similar in mammalian cells and *Xenopus* oocytes. CALHM1 currents were activated when $[Ca^{2+}]_o$ was reduced from 5 mM to 0 mM in the presence of 2 mM Mg^{2+}, whereas reducing $[Ca^{2+}]_o$ from 5 mM to 2 mM in the absence of Mg^{2+} did not activate the currents. Because the surface charge was more or less equal in the two paradigms, these experimental results indicate that reduced $[Ca^{2+}]_o$ induced inward currents by specific mechanisms unrelated to surface charge screening. These results establish extracellular Ca^{2+} regulation of CALHM1 gating as the biophysical basis for the Ca^{2+}-addback response observed in CALHM1-expressing cells.

CALHM1 currents were not inhibited by blockers of voltage-gated Na^+ (10 μM tetrodotoxin), K^+ (10 mM TEA), or Ca^{2+} (1 mM verapamil, 100 μM nifedipine) channels (Fig. 3 *A* and *B*). Similar to CALHM1, connexons can be activated by removal of extracellular Ca^{2+}. However, neither 1-octanol (1 mM) nor carbenoxolone (200 μM), inhibitors of pannexins and connexons, inhibited CALHM1 currents. Inhibitors of NMDAR (100 μM MK-801, 100 μM memantine) were also without effect. Gd^{3+} (100 μM), Ruthenium Red (20 μM), and Zn^{2+} (20 μM) inhibited CALHM1 currents, whereas 1 mM 2-aminoethoxydiphenyl bo-

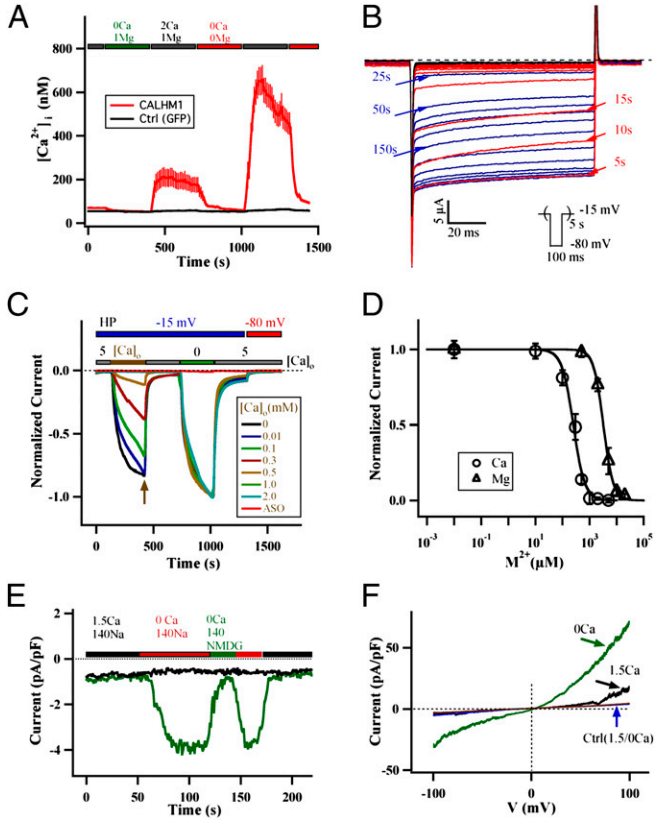

Fig. 2. CALHM1 channels are activated by reduced extracellular Ca^{2+} concentration. (*A*) Removal and subsequent addback of extracellular Ca^{2+} causes rise of $[Ca^{2+}]_i$ in N2A cells transiently transfected with human CALHM1, but not in control GFP-transfected cells. Traces are mean ± SEM of three independent experiments. (*B*) CALHM1 currents, measured every 5 s by a test pulse to −80 mV for 100 ms from a holding potential of −15 mV, increased during continuous perfusion with divalent cation-free solution (0.5 mM EGTA/0.5 mM EDTA) (blue) and reversed to control levels (black) following perfusion with 5 mM Ca^{2+}_o (red). Parentheses indicate voltage pulse protocol repeated every 5 s. (*C*) Time course of CALHM1 current development measured as in *B* by exposure to various bath Ca^{2+} concentrations. Currents were normalized to those at the end of exposure to divalent cation-free solution in each experiment. ASO refers to control oocytes injected only with Cx38 antisense oligonucleotide. (*D*) Ca^{2+}_o (○) and Mg^{2+}_o (△) concentration dependencies of CALHM1 currents measured as in *C*. Data were taken at the end of exposure to various $[Ca^{2+}]_o$ concentrations, indicated by an arrow in *C*. For Ca^{2+}, IC_{50} = 221 ± 21 μM, n_H = 2.1 ± 0.3; for Mg^{2+}, IC_{50} = 3.26 ± 0.25 mM, n_H = 2.3 ± 0.2. *n* = 4–6 experiments at each concentration. (*E*) Whole-cell currents measured in control GFP- (black) (*n* = 4) and CALHM1 (green) (*n* = 5)-expressing N2A cells by 10-ms pulse to −80 mV from holding potential of −40 mV every 1 s in presence and absence of extracellular Ca^{2+} and Na^+ after 12 h transfection. Data were obtained immediately after the capacity current transients. (*F*) Whole-cell currents measured in control GFP- and CALHM1-expressing N2A cells by a voltage-ramp protocol from −100 to +100 mV over 5 s (the holding potential was −40 mV) in presence (1.5 mM) or absence of extracellular Ca^{2+} with 1 mM Mg^{2+} after 24 h transfection.

rate (2-APB) was a partial inhibitor. Flufenamic acid (200 μM) was without effect, whereas niflumic acid (200 μM) partially stimulated CALHM1 currents. These pharmacological properties are unlike those of endogenous oocyte channels or other known ion channels, suggesting that CALHM1 is a unique ion channel with distinctive pharmacology.

CALHM1 Is a Voltage-Gated Ion Channel with an Intrinsic Voltage Sensor. CALHM1 currents exhibit outward rectification in physiological divalent cation-containing solutions (Fig. 1*A*). Rectification could be caused by voltage-dependent pore block by di-

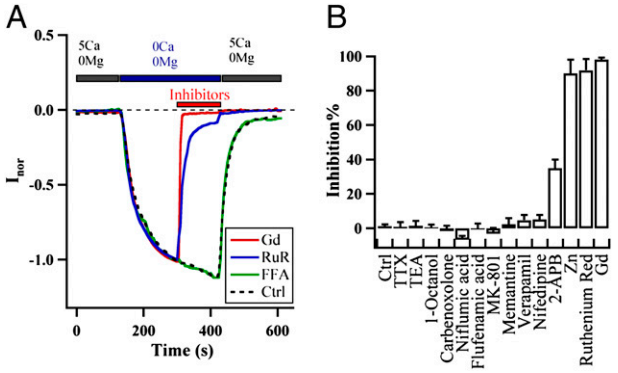

Fig. 3. Pharmacological sensitivities of CALHM1 channel currents. (*A*) Protocol for evaluating pharmacologic sensitivities. CALHM1 currents activated by exposure to nominally divalent-free bath were measured during test pulses to −80 mV (the holding potential was −15 mV). Test agents were perfused into the bath. Shown are inhibition by 100 μM Gd^{3+} (solid red line) and 20 μM ruthenium red (RuR, solid blue line) and no inhibition by 200 μM flufenamic acid (FFA, solid green line), similar to control (without any inhibitor, dashed line). Currents were normalized to those immediately preceding application of drugs. (*B*) Summary of pharmacological responses: TTX (tetrodotoxin, 10 μM), TEA (10 mM), 1-octanol (1 mM), carbenoxolone (200 μM), niflumic acid (200 μM), flufenamic acid (200 μM), MK-801 (100 μM), memantine (100 μM), verapamil (1 mM), nifedipine (100 μM), 2-ABP (1 mM), Zn^{2+} (20 μM), ruthenium red (20 μM), and Gd^{3+} (100 μM). *n* = 3–5, mean ± SEM.

valent cations or it could reflect an intrinsic voltage-dependent gating mechanism. To address the mechanism of voltage dependence, we first asked whether Ca^{2+} acts as a fast voltage-dependent blocker. CALHM1 was activated by depolarization to +60 mV for 3 s, and then the voltage was stepped to various test potentials in either the absence or the presence of Ca^{2+}_o (Fig. 4*A*). The instantaneous current–voltage (I-V) relations were linear in both situations (Fig. 4*B*), suggesting that voltage-dependent gating is not mediated by fast voltage-dependent pore block by extracellular Ca^{2+}. To examine this further, single CALHM1 channel currents were recorded from excised inside-out patches with either 0 or 2 mM Ca^{2+} in the pipette solution at a holding potential of −40 mV. Two mM Ca^{2+} should be saturating at this holding potential. The single-channel current amplitude was unaffected by extracellular Ca^{2+} at a test potential of −80 mV (Fig. 4*C*) and had a linear I-V relation with an ∼24-pS single-channel conductance in 2 mM Ca^{2+} (Fig. 4 *D* and *E*). Similar channels were not observed in control patches (Fig. S1*F*). These results suggest that the voltage dependence of CALHM1 gating is not mediated by either a fast or a slow extracellular divalent cation pore blockage mechanism.

To determine whether CALHM1 possesses an intrinsic voltage sensor, its conductance–voltage (G-V) relation was obtained by measuring tail currents at −80 mV in the absence of divalent cations (Fig. 5*A*). The G-V relationship was fitted by a Boltzmann function with a half-activation voltage ($V_{0.5}$) of −76 mV and slope of 0.6 *e* (Fig. 5*B*). A similar G-V relationship was observed in CALHM1-expressing oocytes injected with either 10 mM BAPTA or a mixture of 10 mM EGTA and 10 mM EDTA to chelate intracellular divalent cations (Fig. S1*E*), ruling out voltage-dependent pore block by intracellular divalent cations. These results suggest that CALHM1 possesses an intrinsic voltage sensor. To further confirm this conclusion, CALHM1 currents were recorded from excised inside-out macropatches with pipette and bath solutions lacking divalent cations. The reversal potential was near zero in these experiments. The channel open probability P_o was greater at +80 mV than at −80 mV (Fig. 5*C*). Taken together, the results demonstrate that CALHM1 is a

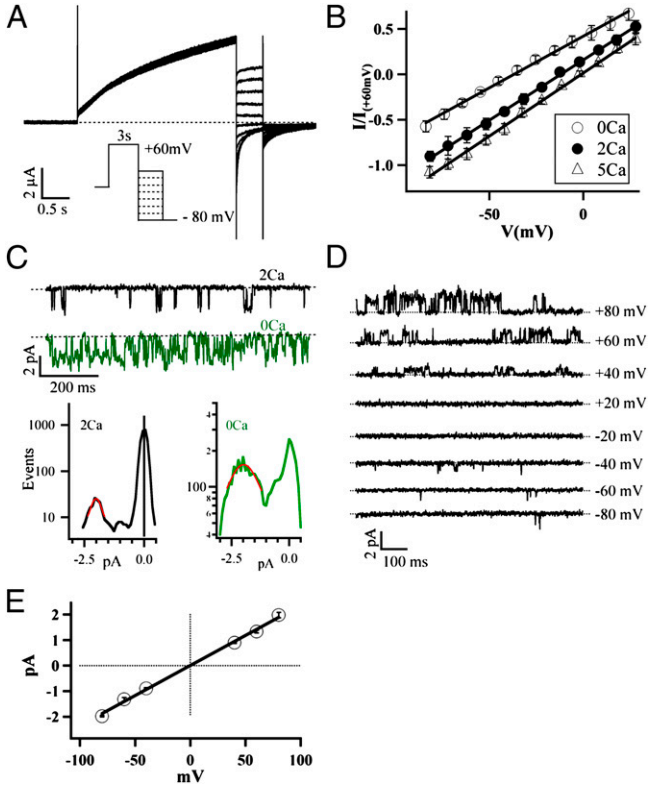

Fig. 4. Voltage-dependent gating of CALHM1 is not due to pore block. (*A*) Instantaneous current–voltage (I-V) protocol and representative current traces in presence of 2 mM Ca^{2+}. Dotted line indicates zero current level. (*B*) Instantaneous I-V relations in different $[Ca^{2+}]_o$. Currents were normalized to those at end of +60 mV prepulse at each $[Ca^{2+}]_o$. Solid lines are linear fits. n = 4–6 experiments at each concentration. (*C*) Excised inside-out patch-clamp recordings of CALHM1 channels in oocyte plasma membranes in presence (2 mM) and absence of Ca^{2+} as indicated. Currents were recorded at −80 mV from a holding potential of −40 mV. Dashed lines indicate channel closed levels. Amplitude histograms obtained from 5-s recordings indicate that single-channel current sizes were similar in presence and absence of $Ca^{2+}{}_o$. (*D*) Single-channel currents recorded from excised inside-out patches from *Xenopus* oocytes with symmetrical Na^+ solutions, 2 mM Ca^{2+} and 1 mM Mg^{2+} in pipette solution, and 11 mM EGTA in bath solution. Representative traces at various voltages from one patch are shown. (*E*) Current–voltage relation for single-channel currents. Mean conductance is 24 ± 0.6 pS. Error bars represent mean ± SEM (n = 4).

weakly voltage-gated channel that possesses a voltage sensor coupled to a gate to open and close it.

Membrane Voltage and Extracellular Calcium Regulation of CALHM1 Are Coupled. Hyperpolarization of the holding potential from −15 mV to −60 mV strongly left shifted the $[Ca^{2+}]_o$ dose–response relation, increasing the apparent Ca^{2+} affinity with IC_{50} = 49 μM and Hill coefficient = 0.80 (Fig. 5*D*). Thus, Ca^{2+} regulation is strongly voltage dependent, with membrane hyperpolarization enhancing the efficacy of extracellular Ca^{2+} to close the channel. It is possible that the Ca^{2+} binding sites may be located in the membrane electric field. However, the different shapes of the $[Ca^{2+}]_o$ dose–response relations between −60 mV and −15 mV holding potentials suggest instead that the conformation of the Ca^{2+} binding sites may be voltage dependent. Extracellular Ca^{2+} slowed outward current activation and accelerated deactivation of the tail currents at −80 mV (Fig. 5*A*). Five mM Ca^{2+} caused a 150-mV depolarizing shift of the G-V relation and increased the voltage dependence without reducing the apparent maximum conductance, G_{max} (Fig. 5*B*). These results indicate that $Ca^{2+}{}_o$ increases the voltage dependence of CALHM1 gating and acts in a voltage-dependent manner to stabilize the CALHM1 channel in closed states. Together, these results indicate that extracellular Ca^{2+} and membrane voltage are allosterically coupled to regulate CALHM1 gating.

Biophysical Properties of WT and P86L CALHM1 Are Similar. A relatively common polymorphism that changes proline at position 86 to leucine (P86L) was suggested to link *CALHM1* to age of onset of Alzheimer's disease (1, 2). Functional studies of populations of suspended cells using the $Ca^{2+}{}_o$ addback protocol suggested that P86L was a partial loss-of-function polymorphism (1). In single-cell imaging of fura-2–loaded N2A cells, we found that P86L-CALHM1 expression was associated with a lower percentage of cells responding with elevated $[Ca^{2+}]_i$ in response to removal of $Ca^{2+}{}_o$ for 5 min and its subsequent addback (Fig. S3*D*). Furthermore, the P86L-CALHM1–expressing cells that did respond had somewhat lower peak $[Ca^{2+}]_i$ elevation compared with WT CALHM1–expressing cells (Fig. S3*C*). Western blot analysis suggested that both CALHM1 forms were expressed at comparable levels (Fig. S3 *A* and *B*). However, we found no differences in the permeation and gating properties between WT and P86L-CALMH1 expressed in *Xenopus* oocytes or N2A cells (Fig. S4). Thus, the P86L polymorphism does not appear to influence the intrinsic biophysical properties of CALHM1 channels.

CALHM1 Regulates Cortical Neuron Excitability. Decreases in $[Ca^{2+}]_o$ increase neuronal excitability in various physiological and pathophysiological settings (10, 11), but the mechanisms are not fully understood. Because CALHM1 is activated by reduced $[Ca^{2+}]_o$ and would contribute a depolarizing excitatory influence, we asked whether CALHM1 participated in low $[Ca^{2+}]_o$-enhanced neuronal excitability. Endogenous CALHM1 protein has not been localized; however, we detected CALHM1 mRNA in both cortical and hippocampal pyramidal neurons, using single-cell mRNA amplification (Fig. S5). Due to its slow gating properties and the lack of specific inhibitors, we have been unable to record endogenous CALHM1 currents in neurons. Alternatively, removal and subsequent addback of $Ca^{2+}{}_o$ elevated $[Ca^{2+}]_i$ much more robustly in primary cultured cortical neurons (PCNs) from WT vs. *CALHM1* knockout (KO) mice (Fig. 6*A*), indicating that endogenous CALHM1 may function in neuronal plasma membranes as it does in heterologous systems. To determine whether CALHM1 channels might be involved in low $[Ca^{2+}]_o$-induced neuronal excitability, we compared electrical responses of PCNs from WT and *CALHM1* KO mice. The bath and pipette solutions contained 1 and 2 mM Mg^{2+} with 4 mM MgATP, respectively, to block TRPM7 channels (12, 13). In response to reduction of $[Ca^{2+}]_o$ from 1.5 to 0.2 mM, input resistance (R_{in}) decreased by ∼50% in WT neurons (Fig. 6*B*), and the cells became more excitable, with smaller current injections required for action potential (AP) generation (Fig. 6*C*). In normal $[Ca^{2+}]_o$, the number of APs generated was a biphasic function of the amount of current injected due to Na^+ channel inactivation at high currents. Exposure to a low level of $[Ca^{2+}]_o$ left shifted the biphasic dependence of the number of APs fired in response to current injection, with the maximal number of APs generated also enhanced (Fig. 6*C*). Strikingly, R_{in} was completely insensitive to reductions of $[Ca^{2+}]_o$ in cortical neurons from *CALHM1* KO mice (Fig. 6*B* and Fig. S6*C*). This observation suggests that CALHM1 contributes significantly to enhanced cortical neuron membrane conductance in reduced $[Ca^{2+}]_o$. Furthermore, reduction of $[Ca^{2+}]_o$ failed to enhance membrane excitability of *CALHM1* KO neurons (Fig. 6 *C* and *E*). In contrast to WT neurons, lowering $[Ca^{2+}]_o$ from 1.5 to 0. 2 mM was without effect on the relationship between the number of APs fired and the magnitude of the stimulus current, nor did it enhance the maximum number of APs generated in *CALHM1* KO neurons

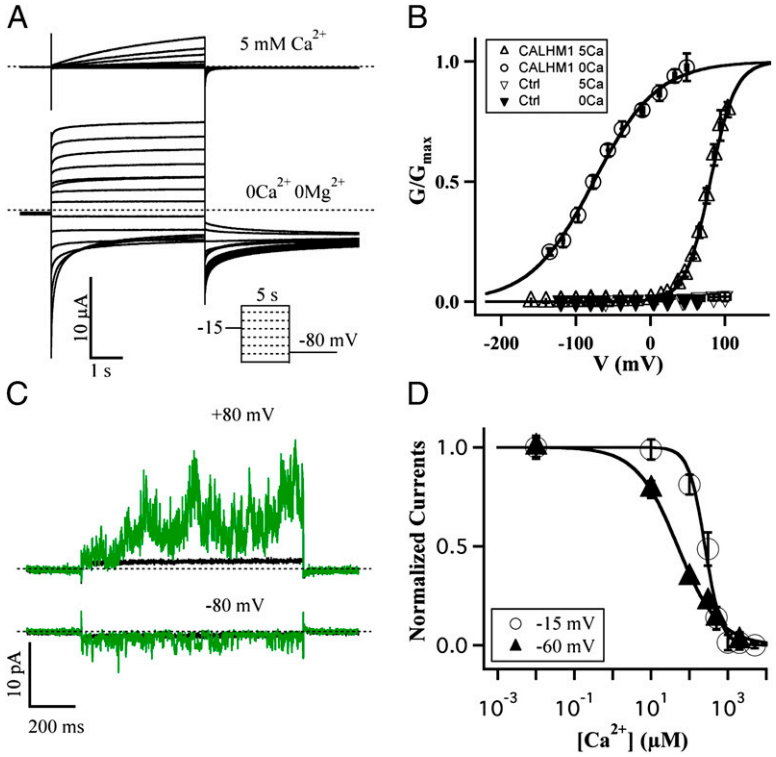

Fig. 5. CALHM1 has an intrinsic voltage-dependent gate. (*A*) CALHM1 currents evoked during 5-s pulses to different voltages from a holding potential of −15 mV in 5 mM Ca^{2+} and divalent cation-free (0-Ca^{2+}, 0-Mg^{2+}) solutions recorded in the same oocyte after continuous perfusion with 0-Ca^{2+} solution for 20 min. Dashed lines indicate zero current levels. (*B*) Conductance–voltage (G-V) relations normalized to G_{max} determined in 0-Ca^{2+}_o solution fitted by Boltzmann functions (lines) [0-Ca^{2+} (○), $V_{0.5}$ = −76 ± 5 mV, Z_e = 0.6 ± 0.05, n = 6; 5 mM Ca^{2+} (△), $V_{0.5}$ = +82 ± 3 mV, Z_e = 1.5 ± 0.05, n = 10]. Currents recorded in control oocytes in 0-Ca^{2+} (▼) and 5 mM Ca^{2+} (▽) solutions were normalized to average currents from CALHM1-expressing oocytes in 0-Ca^{2+}_o from the same batch of oocytes. The normalizations and Boltzmann function fitting were based on the observations in Fig. 4 *C* and *E*. Ca^{2+}_o did not affect the channel conductance. (*C*) Representative current traces (n = 4) recorded from inside-out patch at +80 mV and then at −80 mV from a holding potential of 0 mV in divalent cation-free solution for CALHM1 (green traces) and control (black traces). (*D*) Ca^{2+}_o concentration dependencies of CALHM1 currents measured as in Fig. 2*C* from −15-mV (○) and −60-mV (▲) holding potentials, respectively, fitted with Hill equations (−15 mV, IC_{50} = 221 ± 21 μM, n_H = 2.1 ± 0.3; −60 mV, IC_{50} = 49 ± 4 μM, n_H = 0.80 ± 0.05). n = 4–6 experiments at each concentration.

(Fig. 6*C*). Thus, enhanced cortical neuron excitability in response to reduced $[Ca^{2+}]_o$ is absent in *CALHM1* knockout cells. These results suggest that CALHM1 mediates low $[Ca^{2+}]_o$-induced excitability of cortical neurons.

Surprisingly, the current required to hold cortical neurons at −75 mV (I_{Hold}) was unexpectedly larger in the KO neurons than in WT neurons in 1.5 mM Ca^{2+} (−44.0 ± 4.3 vs. −23.3 ± 4.5 pA for KO and WT cells, respectively; Fig. S6*A*) although the resting membrane potential and cell size (membrane capacitance) were not different (Fig. S6*A*). Accordingly, *CALHM1* KO cells had diminished R_{in} (Fig. S6 *B* and *C*) and required nearly twofold greater current injection (500-ms pulses) to elicit AP firing (Fig. 6 *C* and *E*). As the magnitude of the injection current was increased, the number of APs generated by WT neurons increased to a peak (~4 APs) and then declined, presumably due to Na^+ channel inactivation (Fig. 6 *C* and *D*). Neurons from KO animals had a higher AP ceiling, approximately twice that observed in WT neurons, which did not diminish with stronger stimulation (Fig. 6 *C* and *E*). Whereas the evoked APs in both populations had similar thresholds, overshoots, and half-widths (Fig. S7 *A* and *B*), the relaxation kinetics of the after-hyperpolarization (AHP) were markedly prolonged in the KO cells (Fig. 6*E* and Fig. S7*C*). Thus, *CALHM1* knockout alters cortical neuronal electrical properties, rendering the cells less excitable at low input stimulus strength, but transforming them from phasic to tonic responders with stronger depolarizing inputs. Nevertheless, the main finding in this study is that CALHM1 mediates low $[Ca^{2+}]_o$-induced excitability of cortical neurons.

Discussion

Our results demonstrate that CALHM1 is a neuronal Ca^{2+}-permeable plasma membrane ion channel with unusual permeability properties and gating regulation by both membrane voltage and extracellular $[Ca^{2+}]$. Furthermore, we show that its regulation by extracellular Ca^{2+} has physiological relevance by demonstrating that CALHM1 mediates enhanced excitability of cortical neurons in response to reductions of $[Ca^{2+}]_o$. That CALHM1 is itself an ion channel was suggested by the similar properties of the unique ion currents observed in CALHM1-expressing *Xenopus* oocytes and a mammalian neuroblastoma cell line. The identification of a single residue that when mutated changed the selectivity properties of the CALHM1-associated currents establishes CALHM1 as the pore-forming subunit of a unique Ca^{2+}-permeable voltage-gated ion channel.

The CALHM1 channel has unusual ion selectivity and gating regulation properties. It is Ca^{2+} permeable, with a modest selectivity for Ca^{2+} over monovalent cations, but it demonstrates little selectivity among monovalent cations or even between monovalent cations and chloride. Thus, when CALHM1 is activated, the current carried through the channel is a mixture of Na^+, K^+, Cl^-, and Ca^{2+}, and its activation is predicted to be a depolarizing, excitatory influence on membrane properties (1, 6). Mutation of an aspartic acid residue located at the presumed extracellular end of TM3 in CALHM1 strongly affected the Ca^{2+} selectivity. The importance of this residue for Ca^{2+} selectivity is likely due to its acidic nature, because substitution with glutamate to preserve the charge had little or no effect on Ca^{2+} selectivity.

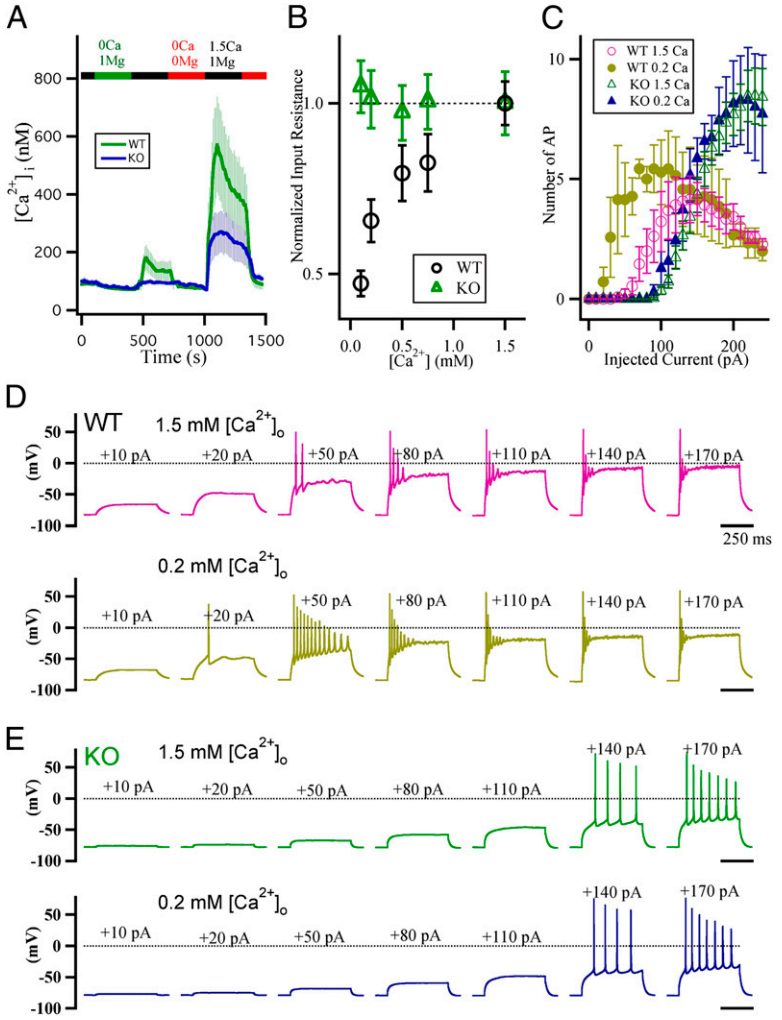

Fig. 6. CALHM1 regulates cortical neuron excitability and responses to reduced extracellular Ca^{2+} concentrations. (*A*) Reducing $[Ca^{2+}]_o$ activates a CALHM1-mediated plasma membrane Ca^{2+} influx pathway in cortical neurons. Removal and subsequent addback of extracellular Ca^{2+} cause rise of $[Ca^{2+}]_i$ in mouse primary cultured cortical neurons that was muted in cortical neurons from *CALHM1* knockout mice. Traces are mean ± SEM of three independent experiments. Slower relaxation kinetics of $[Ca^{2+}]_i$ to control levels after reintroduction of extracellular Ca^{2+} compared with CALHM1 currents (here and in Fig. 2*A*) are likely due to incomplete closure of CALHM1 upon reintroduction of extracellular Ca^{2+} in the imaging experiments due to CALHM1-activation–induced depolarization. (*B*) Input resistances for WT and KO in various $[Ca^{2+}]_o$ obtained by linear fits to data of the membrane-potentials vs. injected-currents relations and further normalized by value at 1.5 mM for WT (723 ± 46 MΩ, n = 8) and KO (253 ± 19 MΩ, n = 15), respectively. Dashed line represents value of 1. Representative data are shown in Fig. S6C. Error bars show mean ± SEM. (*C*) Numbers of overshooting action potentials during 500-ms depolarizing current injections in WT (n = 12) and KO (n = 15) neurons in 1.5 or 0.2 mM $Ca^{2+}{}_o$. (*D* and *E*) Representative current-clamp recordings from (*D*) WT (I_{Hold} = −15 pA) and (*E*) *CALHM1* KO (I_{Hold} = −50 pA) neurons in solutions containing 1.5 mM (*Upper*) and 0.2 mM (*Lower*) Ca^{2+} at various depolarizing current injections. Dashed lines represent 0 mV.

We demonstrate that CALHM1 is a voltage-gated channel possessing an intrinsic voltage sensor. However, the molecular basis for voltage-dependent gating is not obvious. CALHM1 has only one basic residue (in putative TM3), unlike other voltage-gated channels, which have several basic residues in an S4 segment. Although the number of basic residues in or near putative transmembrane helices in CALHM1 is small, large-conductance BK voltage-gated K^+ channels contain multiple basic residues, but only one contributes most of the gating charge (14). The important residues involved in voltage sensing in CALHM1, and the nature of the motions of the voltage-sensor domain in response to changes in membrane potential, remain to be identified. In addition to its voltage sensitivity, CALHM1 responds to levels of extracellular Ca^{2+}. Reducing $[Ca^{2+}]_o$ reversibly activates CALHM1 in a concentration- and time-dependent manner by a mechanism involving gating regulation rather than pore block. The $[Ca^{2+}]_o$ regulation of CALHM1 gating is voltage dependent, suggesting that two mechanisms, voltage and $Ca^{2+}{}_o$, are coupled to affect channel gating. The $[Ca^{2+}]_o$ regulation of CALHM1 channel gating can account for the original observations of the effects of CALHM1 expression on cytoplasmic Ca^{2+} homeostasis (1). In those studies, repeated here in different cell types, removal of extracellular Ca^{2+} strongly enhanced the plasma membrane Ca^{2+} permeability, as revealed by an immediate very large rise of $[Ca^{2+}]_i$ upon $Ca^{2+}{}_o$ addback. It is now clear that removal of $Ca^{2+}{}_o$ activated CALHM1, and readdition of Ca^{2+} to the medium enabled Ca^{2+} to permeate through CALHM1 into the cytoplasm before $Ca^{2+}{}_o$ could close the channel. The observed delay in return to basal $[Ca^{2+}]_i$ when $Ca^{2+}{}_o$ was restored is most likely accounted for by CALHM1 activation-induced depolarization that enables CALHM1 to remain partially active in nonvoltage-clamped cells. This mechanism does not appear to involve store-operated Ca^{2+} entry (SOCE), because store depletion and CALHM1 activation pro-

duced additive effects on Ca^{2+} influx (Fig. S8*A*). Furthermore, elevated $[Ca^{2+}]_i$ in response to Ca^{2+} addback in CALHM1-expressing cells was normal in 293 cells stably expressing a dominant-negative ORAI1 channel that blocks SOCE (Fig. S8*B*).

The P86L polymorphism identified in *CALHM1* has been shown most recently to not be an independent risk factor for Alzheimer's disease, although it may influence age of onset (2). It has been suggested that P86L-CALHM1 has partial loss of function (1, 9). However, we could not find any differences in the biophysical and regulatory properties of P86L- vs. WT-CALHM1 channels. It was previously suggested that this polymorphism reduced modestly the Ca^{2+} selectivity of currents observed in CALHM1-expressing CHO cells (1). However, CALHM1 current densities were low and therefore likely contaminated by endogenous currents present even with internal Cs^+ and external 100 mM NMDG. In addition, a slow voltage ramp was used to determine the reversal potential in the previous study, which, because of the voltage and extracellular Ca^{2+} dependence of CALHM1 gating discovered here, may have caused time-dependent changes in its contribution to the total membrane currents, introducing errors into the reversal potential determinations. Thus, the currents recorded previously likely had errors associated with them that do not exist in the present study that used instantaneous voltage pulse protocols. Our results suggest that the observed reduced response to Ca^{2+} addback of P86L-CALHM1–expressing cells is unlikely to be caused by alterations of CALHM1 channel properties. In our analyses of the responses of single cells to the Ca^{2+} addback protocol, we did note, however, that significantly fewer of the P86L- vs. WT-CALHM1–expressing cells responded, and of those that responded, the average $[Ca^{2+}]_i$ response of the P86L-expressing cells was smaller. Because both isoforms were expressed at similar levels, these results taken together suggest that the P86L polymorphism may influence the amount of CALHM1 at the plasma membrane or regulatory mechanisms (e.g., protein interactions) that are lacking in *Xenopus* oocytes.

Knockout of *CALHM1* eliminated low-$[Ca^{2+}]_o$–induced cortical neuron excitability and it altered basal cortical neuronal electrical properties. However, the changes observed—decreased input resistance and transition of neuronal firing from phasic to tonic—are unexpected on the basis of simple loss of CALHM1 conductance. The altered properties in the KO neurons could be due to enhanced expression of K^+ conductance(s) that contributes to diminished R_{in} and sensitivity of AP firing to depolarizing stimuli, as well as enhanced duration of the AHP that results in the ability of the neurons to maintain tonic AP generation at higher stimulus strengths. Why cells lacking CALHM1 display these properties is unclear.

Importantly, however, we established an essential role for CALHM1 in cortical neuronal responses to reduced extracellular Ca^{2+} concentrations. Mouse cortical neurons respond to reduced $[Ca^{2+}]_o$ with enhanced membrane conductance and excitability, but these responses are nearly completely absent in mice with *CALHM1* deleted. Our results therefore indicate that gating of CALHM1 by extracellular Ca^{2+} mediates the electrophysiological responses of cortical neurons to reduced $[Ca^{2+}]_o$ that could be importantly involved in responses to changes in $[Ca^{2+}]_o$ in the central nervous system. Normal and pathophysiological electrical activity can result in modest to substantial reductions (to <0.1 mM) in $[Ca^{2+}]_o$ in the interstitium and synaptic clefts in the brain, even following a single presynaptic action potential (15–26), well within the range of CALHM1 activation determined here. Profound reductions of $[Ca^{2+}]_o$ have been observed in spreading depression, anoxia, seizures, and traumatic injury that cause massive release of glutamate and activation of postsynaptic Ca^{2+} influx pathways (10, 27–30). Decreases in $[Ca^{2+}]_o$ have been observed to increase electrical excitability in various physiological and pathophysiological settings (21, 31, 32), but the mechanisms are not fully understood or accounted for. Two ion channels have been identified that might contribute to such responses. NALCN, a Na^+ leak channel (33) with minimal Ca^{2+} permeability, is activated in hippocampal pyramidal cells indirectly by low $[Ca^{2+}]_o$ by a G-protein–coupled receptor (11). TRPM7 can also be activated in hippocampal neurons under conditions in which divalent cation concentrations fall, although normal intracellular Mg^{2+} levels are expected to minimize such activation (34). In contrast, CALHM1 is regulated in cortical neurons by $[Ca^{2+}]_o$ directly, in a process that is coupled to an intrinsic voltage-dependent gating mechanism. In addition, CALHM1 has a considerable Ca^{2+} permeability. These properties distinguish CALHM1 from these other channels and suggest that it could be important in neuronal activities for which mechanisms are still unclear, for example fast activity-dependent modulation of neurotransmission (23) and the "Ca^{2+} paradox" associated with neuronal death during excitotoxic stimulation (10, 34). The Ca^{2+} paradox describes a phenomenon observed in heart and neurons (including hippocampus) (10, 35, 36) in which exposure of cells to reduced $[Ca^{2+}]_o$, as can occur during periods of high levels of excitability, including seizures and anoxia, leads to increased $[Ca^{2+}]_i$, particularly when $[Ca^{2+}]_o$ is restored to normal levels, the latter often constituting a toxic insult (10, 37–39). Various mechanisms have been proposed to account for these observations (10). Identification of CALHM1 as a Ca^{2+}-permeable channel activated by depolarization and reduced $[Ca^{2+}]_o$ suggests that it could be a prime candidate to contribute to such phenomena.

Experimental Procedures

Cell Culture, Transfection, and Western Blotting. Primary cultured cortical neurons were prepared from embryonic day 15 (E15–16) mice, as described in ref. 40. Briefly, cortical neurons were isolated by digestion with papain and plated on poly-L-lysine–coated glass coverslips (12 mm diameter) in 35-mm dishes at ~2×10^5 cells per dish in 80% (vol/vol) DMEM (BioWhittaker), 10% (vol/vol) Ham's F-12 (BioWhittaker), 10% (vol/vol) bovine calf serum (iron supplemented; HyClone), and 0.5× penicillin/streptomycin (Invitrogen). The medium was changed the next day [days in vitro (DIV) 1] to Neurobasal A medium (GIBCO) supplemented with 2% (vol/vol) B-27, 0.5× penicillin/streptomycin, and 1× Glutamax. Cultures were maintained at 37 °C in a humidified incubator at 5% CO_2. When necessary, cytosine-arabinofuranosiude (ARAc) (Sigma) was added at 5 μM to suppress glial growth. Neurons between DIV 7 and 12 were used in imaging and electrophysiological recordings. At least 1 d before experiments, two-thirds of the medium was replaced with fresh medium without ARAc and antibiotics. The N2A mouse neuroblastoma cell line was cultured in Eagle's minimum essential medium supplemented with 10% FBS and 0.5× penicillin/streptomycin (Invitrogen) at 37 °C, 5% CO_2. N2A cells were plated onto glass coverslips coated with poly-L-lysine (Sigma) 1 d before transfection. Sixteen hours posttransfection, cells were lysed and 40 μg of total protein was run on a 10% Tris-Acetate SDS/PAGE gel. The gel was transferred to nitrocellulose membrane and probed with an antibody against CALHM1. The gel was then stripped (Restore Western blot stripping buffer; Pierce) and reprobed with an antibody directed against β-tubulin.

***Xenopus* Oocyte Electrophysiology.** cRNA was in vitro transcribed from linearized plasmids with the mMessage mMachine kit (Ambion). Female *Xenopus laevis* were purchased from *Xenopus* One. Oocytes were defolliculated by treatment with collagenase (Worthington Biochemical). At least 2 h after collagenase treatment, 1–5 ng of CALHM1 cRNA was injected into oocytes with 80 ng of *Xenopus* connexin-38 antisense oligonucleotide to inhibit endogenous Cx38 currents (Fig. S1*A*). Oocytes were kept at 16 °C in an ND96 solution: 96 mM NaCl, 2 mM KCl, 1.8 mM $CaCl_2$, 1 mM $MgCl_2$, 2.5 mM Na-pyruvate, 1× penicillin/streptomycin, at pH 7.6 (adjusted by NaOH). Recordings were performed at room temperature (20–23 °C) 3–5 d after injection. Oocytes used in two-electrode voltage-clamp experiments were injected with a 50-nL mixture of 20 mM BAPTA and 10 mM Ca^{2+} at least 30 min before recording to clamp $[Ca^{2+}]_i$ to ~100 nM and minimize activation of endogenous Ca^{2+}-activated Cl^- currents (Fig. S1*B*). In two-electrode voltage-clamp experiments, currents were recorded in a standard bath solution containing 100 mM Na^+, 100 mM Cl^-, 2 mM K^+, and 10 mM Hepes, pH 7.2 adjusted with methanesulfonic acid, with various concentrations of Ca^{2+} and Mg^{2+}. Usually no divalent cation buffers were added, except in the 10-μM

Ca^{2+} solution that contained 5 mM HEDTA. Calculation of free Ca^{2+} concentration was done with WEBMAXC software. In divalent cation-free solutions, 0.5 mM EGTA and 0.5 mM EDTA were added to the standard bath solution without adding divalent cations. Nominally divalent cation-free solutions were prepared by addition of neither divalent cations nor buffers. In ion permeability experiments, sucrose was used as a substitute for NaCl or Ca^{2+}. Data were acquired with an OC-725C amplifier (Warner Instrument) at 1 kHz with a 16-bit A/D converter (Instrutech ITC-16). Traces recorded in 100 μM Gd^{3+} were used for leak subtraction. Electrodes were made from thin-walled TW100F-6 glass (World Precision Instruments), filled with 3 M KCl, connected by 3 M KCl agar bridges to the bath solution. In excised inside-out patch experiments, the pipette solution contained 160 mM Na^+, 10 mM Cl^-, and 10 mM Hepes, pH 7.2 adjusted by methanesulfonate. Divalent cation-free solutions contained 0.5 mM EGTA and 0.5 mM EDTA; physiological solutions contained 2 mM Ca^{2+} and 1 mM Mg^{2+}. The bath solution contained 160 mM Na^+, 10 mM Cl^-, 11 mM EGTA, and 10 mM Hepes, pH 7.2 adjusted by methanesulfonate. Data were acquired with an Axopatch 200B amplifier in patch mode at 5 kHz. Currents were filtered by an eight-pole Bessel filter (Frequency Devices) at 1 kHz and sampled at 5 kHz with an 18-bit A/D converter (Instrutech ITC-18). Electrodes were made from thick-walled PG10150-4 glass (World Precision Instruments) coated with wax.

Relative permeabilities of K^+, Cl^-, and Na^+ (P_K/P_{Na} and P_{Cl}/P_{Na}) were estimated from reversal potentials (E_{rev}), using the GHK constant field equation

$$E_{rev} = \frac{RT}{F} \ln \frac{P_K[K^+]_o + P_{Na}[Na^+]_o + P_{Cl}[Cl^-]_i}{P_K[K^+]_i + P_{Na}[Na^+]_i + P_{Cl}[Cl^-]_o},$$

where subscripts i and o denote intracellular and extracellular, respectively; R, T, and F have their usual meanings; and P_{Na}, P_K, and P_{Cl} are the membrane permeabilities to Na^+, K^+, and Cl^-, respectively. For estimations of the relative Ca^{2+} permeability, the GHK equation can be derived to an extended constant-field equation without any assumptions,

$$E_{rev} = \frac{RT}{F} \ln \frac{-b + \sqrt{b^2 - 4ac}}{2a},$$

where

$$a = [Na^+]_i + \frac{P_K}{P_{Na}}[K^+]_i + 4\frac{P_{Ca}}{P_{Na}}[Ca^{2+}]_i + \frac{P_{Cl}}{P_{Na}}[Cl^-]_o$$

$$b = ([Na^+]_i - [Na^+]_o) + \frac{P_K}{P_{Na}}([K^+]_i - [K^+]_o) - \frac{P_{Cl}}{P_{Na}}([Cl^-]_i - [Cl]_o^-)$$

$$c = -[Na^+]_o - \frac{P_K}{P_{Na}}[K^+]_o - \frac{P_{Cl}}{P_{Na}}[Cl^-]_i - 4\frac{P_{Ca}}{P_{Na}}[Ca^{2+}]_o$$

and P_{Na}, P_K, P_{Cl}, and P_{Ca} are the membrane permeabilities to Na^+, K^+, Cl^-, and Ca^{2+}, respectively.

N2A Cell Electrophysiology. Whole-cell currents were recorded at room temperature 16–24 h after transfection. The pipette solution contained 140 mM CsF, 6 mM $MgCl_2$, 1 mM $CaCl_2$, 11 mM EGTA, 2 mM TEA^+, and 10 mM Hepes, pH 7.3 adjusted by methanesulfonic acid, ~308 mOsm. Bath solutions contained 145 mM Na^+, 5.4 mM K^+, 10 mM TEA^+, 0.001 mM TTX, 10 mM glucose, 1.5 mM Ca^{2+}, 1 mM Mg^{2+}, 150 mM Cl^-, and 10 Hepes, pH 7.4 adjusted by methanesulfonic acid, ~330 mOsm. TEA^+ and TTX do not block CALHM1 currents (Fig. 3*B*). In 0-Na^+ bath, Na^+ was replaced by $NMDG^+$. A Ca^{2+}-free bath solution included 0.5 mM EGTA without added Ca^{2+}. Data were acquired with an Axopatch 200B amplifier in whole-cell mode at 5 kHz. Currents were filtered by an eight-pole Bessel filter at 1 kHz and sampled at 5 kHz with an 18-bit A/D converter. Electrodes were made from thick-walled PG10150-4 glass.

Mouse Cortical Neuron Electrophysiology. Cultured pyramidal cortical neurons were identified morphologically and confirmed as such by expression of the neuronal marker MAP2 (Fig. S5). For whole-cell current-clamp recordings, the pipette solution contained 140 mM K^+, 5 mM Na^+, 2 mM Mg^{2+}, 10 mM Cl^-, 1 mM EGTA, 4 mM MgATP, 0.3 mM Tris·GTP, 14 mM phosphocreatine (di-Tris salt), and 10 mM Hepes, pH 7.3 adjusted by methanesulfonic acid, ~290 mOsm. The bath solution contained 150 mM Na^+, 5.4 mM K^+, 1 mM Mg^{2+}, 150 mM Cl^-, 20 mM glucose, 10 mM Hepes, and 1.5 mM Ca^{2+} (unless otherwise indicated), pH 7.4 adjusted by methanesulfonate, ~330 mOsm. These solutions are similar to those used in other current-clamp studies (11, 36). Data acquisition was as described above for N2A cell whole-cell voltage-clamp experiments. Current-clamp experiments were performed alternately on the same day on cells from WT and KO mice from DIV 7 to 12.

Single-Cell Ca^{2+} Imaging. $[Ca^{2+}]_i$ was measured in transfected N2A and PC12 cells and cortical neurons that were plated on poly-L-lysine–coated glass coverslips. Cell were loaded with Fura-2 by incubation in a medium containing 2 μM Fura-2-AM for 25–30 min, followed by 5 min continuous perfusion with dye-free solution. Fura-2 fluorescence imaging was performed as described in ref. 41. The ratio of emitted light at 520 ± 20 nm upon excitation with 340 ± 5 nm and 380 ± 5 nm light was used to determine $[Ca^{2+}]_i$ with a Perkin-Elmer Ultraview imaging system. N2A and PC12 cells were used 16–24 h after transfection, and cortical neurons were used between DIV 7 and 12.

CALHM1 Knockout Mice. *CALHM1* knockout mice were developed in the P.M. laboratory. The generation of the *CALHM1*$^{+/-}$ (heterozygous KO) founder mice was outsourced to genOway. Briefly, a strategy consisting of deleting 552 bp of *CALHM1* coding sequences containing the ATG start codon and the entire exon 1 was chosen. *CALHM1* deletion was performed by homologous recombination in cells, using the PMA1-HR targeting vector (genOway). The targeting vector was electroporated into 129Sv embryonic stem (ES) cells and 307 resistant ES cell clones were isolated, screened by PCR, and confirmed by Southern blot analysis to unambiguously confirm the 5′- and 3′-targeting events. Selected ES clones were injected into C57BL/6J blastocytes and reimplanted into OF1 pseudopregnant females. Male chimeras presenting a high chimerism rate were then mated with WT C57BL/6J females. *CALHM1*$^{+/+}$ and *CALHM1*$^{-/-}$ mice were derived by cross-mating between *CALHM1*$^{+/-}$ founder mice. *CALHM1*$^{-/-}$ mice were viable and obtained with a normal Mendelian inheritance of the mutant *CALHM1* allele, ruling out an essential function of CALHM1 in mouse embryogenesis. The *CALHM1*$^{+/+}$ and *CALHM1*$^{-/-}$ mice were then bred independently of one another to generate pups for primary neuronal cultures.

ACKNOWLEDGMENTS. We thank Lijuan Mei and Jun Yang for molecular biology assistance; Dr. Akiyuki Taruno for mice assistance; Drs. Donald Gill and Youjun Wang for the dominant-negative Orai1 HEK293 stable cell line; and Drs. Todd Lamitina, Jessica Tanis, Horia Vais, and Dejian Ren for helpful discussions. This work was supported by grants from the American Health Assistance Foundation (to J.K.F.) and National Institutes of Health Grants MH059937 (to J.K.F.) and HD059288 and NS069629 (to A.S.C.).

1. Dreses-Werringloer U, et al. (2008) A polymorphism in CALHM1 influences Ca^{2+} homeostasis, Abeta levels, and Alzheimer's disease risk. *Cell* 133:1149–1161.
2. Lambert JC, et al. (2010) The CALHM1 P86L polymorphism is a genetic modifier of age at onset in Alzheimer's disease: A meta-analysis study. *J Alzheimers Dis* 22:247–255.
3. Ebihara L (1996) Xenopus connexin38 forms hemi-gap-junctional channels in the nonjunctional plasma membrane of Xenopus oocytes. *Biophys J* 71:742–748.
4. Bahima L, et al. (2006) Endogenous hemichannels play a role in the release of ATP from Xenopus oocytes. *J Cell Physiol* 206:95–102.
5. Sather WA, McCleskey EW (2003) Permeation and selectivity in calcium channels. *Annu Rev Physiol* 65:133–159.
6. Owsianik G, Talavera K, Voets T, Nilius B (2006) Permeation and selectivity of TRP channels. *Annu Rev Physiol* 68:685–717.
7. Prakriya M, et al. (2006) Orai1 is an essential pore subunit of the CRAC channel. *Nature* 443:230–233.
8. Zhou Y, Ramachandran S, Oh-Hora M, Rao A, Hogan PG (2010) Pore architecture of the ORAI1 store-operated calcium channel. *Proc Natl Acad Sci USA* 107:4896–4901.
9. Moreno-Ortega AJ, Ruiz-Nuño A, García AG, Cano-Abad MF (2010) Mitochondria sense with different kinetics the calcium entering into HeLa cells through calcium channels CALHM1 and mutated P86L-CALHM1. *Biochem Biophys Res Commun* 391: 722–726.
10. MacDonald JF, Xiong ZG, Jackson MF (2006) Paradox of Ca^{2+} signaling, cell death and stroke. *Trends Neurosci* 29:75–81.
11. Lu B, et al. (2010) Extracellular calcium controls background current and neuronal excitability via an UNC79-UNC80-NALCN cation channel complex. *Neuron* 68:488–499.
12. Prakriya M, Lewis RS (2002) Separation and characterization of currents through store-operated CRAC channels and Mg^{2+}-inhibited cation (MIC) channels. *J Gen Physiol* 119:487–507.
13. Kozak JA, Cahalan MD (2003) MIC channels are inhibited by internal divalent cations but not ATP. *Biophys J* 84:922–927.
14. Ma Z, Lou XJ, Horrigan FT (2006) Role of charged residues in the S1-S4 voltage sensor of BK channels. *J Gen Physiol* 127:309–328.
15. Benninger C, Kadis J, Prince DA (1980) Extracellular calcium and potassium changes in hippocampal slices. *Brain Res* 187:165–182.
16. Heinemann U, Pumain R (1980) Extracellular calcium activity changes in cat sensorimotor cortex induced by iontophoretic application of aminoacids. *Exp Brain Res* 40:247–250.

17. Krnjević K, Morris ME, Reiffenstein RJ (1982) Stimulation-evoked changes in extracellular K^+ and Ca^{2+} in pyramidal layers of the rat's hippocampus. *Can J Physiol Pharmacol* 60:1643–1657.
18. Krnjević K, Morris ME, Reiffenstein RJ, Ropert N (1982) Depth distribution and mechanism of changes in extracellular K^+ and Ca^{2+} concentrations in the hippocampus. *Can J Physiol Pharmacol* 60:1658–1671.
19. Nicholson C, Bruggencate GT, Steinberg R, Stöckle H (1977) Calcium modulation in brain extracellular microenvironment demonstrated with ion-selective micropipette. *Proc Natl Acad Sci USA* 74:1287–1290.
20. Pumain R, Heinemann U (1985) Stimulus- and amino acid-induced calcium and potassium changes in rat neocortex. *J Neurophysiol* 53:1–16.
21. Pumain R, Kurcewicz I, Louvel J (1983) Fast extracellular calcium transients: Involvement in epileptic processes. *Science* 222:177–179.
22. Borst JG, Sakmann B (1999) Depletion of calcium in the synaptic cleft of a calyx-type synapse in the rat brainstem. *J Physiol* 521:123–133.
23. Rusakov DA, Fine A (2003) Extracellular Ca^{2+} depletion contributes to fast activity-dependent modulation of synaptic transmission in the brain. *Neuron* 37:287–297.
24. Stanley EF (2000) Presynaptic calcium channels and the depletion of synaptic cleft calcium ions. *J Neurophysiol* 83:477–482.
25. Egelman DM, Montague PR (1999) Calcium dynamics in the extracellular space of mammalian neural tissue. *Biophys J* 76:1856–1867.
26. Vassilev PM, Mitchel J, Vassilev M, Kanazirska M, Brown EM (1997) Assessment of frequency-dependent alterations in the level of extracellular Ca^{2+} in the synaptic cleft. *Biophys J* 72:2103–2116.
27. Heinemann U, Konnerth A, Pumain R, Wadman WJ (1986) Extracellular calcium and potassium concentration changes in chronic epileptic brain tissue. *Adv Neurol* 44: 641–661.
28. Morris ME, Trippenbach T (1993) Changes in extracellular $[K^+]$ and $[Ca^{2+}]$ induced by anoxia in neonatal rabbit medulla. *Am J Physiol* 264:R761–R769.
29. Nilsson P, Hillered L, Olsson Y, Sheardown MJ, Hansen AJ (1993) Regional changes in interstitial K^+ and Ca^{2+} levels following cortical compression contusion trauma in rats. *J Cereb Blood Flow Metab* 13:183–192.
30. Silver IA, Erecińska M (1990) Intracellular and extracellular changes of $[Ca^{2+}]$ in hypoxia and ischemia in rat brain in vivo. *J Gen Physiol* 95:837–866.
31. Wang T, Wang J, Cottrell JE, Kass IS (2004) Small physiologic changes in calcium and magnesium alter excitability and burst firing of CA1 pyramidal cells in rat hippocampal slices. *J Neurosurg Anesthesiol* 16:201–209.
32. Xiong ZG, MacDonald JF (1999) Sensing of extracellular calcium by neurones. *Can J Physiol Pharmacol* 77:715–721.
33. Lu B, et al. (2007) The neuronal channel NALCN contributes resting sodium permeability and is required for normal respiratory rhythm. *Cell* 129:371–383.
34. Wei WL, et al. (2007) TRPM7 channels in hippocampal neurons detect levels of extracellular divalent cations. *Proc Natl Acad Sci USA* 104:16323–16328.
35. Burgo A, Carmignoto G, Pizzo P, Pozzan T, Fasolato C (2003) Paradoxical Ca^{2+} rises induced by low external Ca^{2+} in rat hippocampal neurones. *J Physiol* 549:537–552.
36. Xiong Z, Lu W, MacDonald JF (1997) Extracellular calcium sensed by a novel cation channel in hippocampal neurons. *Proc Natl Acad Sci USA* 94:7012–7017.
37. Zimmerman AN, Hülsmann WC (1966) Paradoxical influence of calcium ions on the permeability of the cell membranes of the isolated rat heart. *Nature* 211:646–647.
38. Chinopoulos C, Adam-Vizi V (2006) Calcium, mitochondria and oxidative stress in neuronal pathology. Novel aspects of an enduring theme. *FEBS J* 273:433–450.
39. Deshpande LS, Limbrick DD, Jr., Sombati S, DeLorenzo RJ (2007) Activation of a novel injury-induced calcium-permeable channel that plays a key role in causing extended neuronal depolarization and initiating neuronal death in excitotoxic neuronal injury. *J Pharmacol Exp Ther* 322:443–452.
40. Meberg PJ, Miller MW (2003) Culturing hippocampal and cortical neurons. *Methods Cell Biol* 71:111–127.
41. Foskett JK (1988) Simultaneous Nomarski and fluorescence imaging during video microscopy of cells. *Am J Physiol* 255:C566–C571.